

Synergistic Effects of Nano –Zinc in Nano – Technology and Its Potential Influence on Bacterial Isolation from Women Experiencing Miscarriage

Israa Hameed Abbas¹, Rihab Edan Kadhimi², Shakir H. Mohamed Al- Alwany³

¹Ministry of Health, Babylon Health Department, Iraq

Email ID: israamsc2021@gmail.com

²Department of Biology, College of Science-University of Babylon, Iraq

Email ID: sci.rihab.edan@uobabylon.edu.iq

³Department of Biology, College of Science-University of Babylon, Iraq

Email ID: sci.shakir.hammad@uobabylon.edu.iq

Cite this paper as: Israa Hameed Abbas, Rihab Edan Kadhimi, Shakir H. Mohamed Al- Alwany, (2025) Synergistic Effects of Nano –Zinc in Nano – Technology and Its Potential Influence on Bacterial Isolation from Women Experiencing Miscarriage. *Journal of Neonatal Surgery*, 14 (20s), 432-442.

ABSTRACT

Background: The biological synthesis of zinc oxide nanoparticles (ZnONPs) using *Juglans regia* (walnut) bark extract presents an eco-friendly and sustainable alternative to conventional chemical methods. The phytochemicals present in the plant extract act as natural reducing and stabilizing agents, facilitating the conversion of zinc ions into nanoparticles. This green synthesis not only minimizes environmental impact but also enhances the biological properties of the produced nanoparticles.

Aim of the Study: This study aimed to synthesize ZnONPs biologically using *J. regia* bark extract and evaluate their antibacterial activity against multidrug-resistant bacterial isolates (*Klebsiella* sp., *Escherichia coli*, and *Enterobacter* sp.) obtained from recurrent miscarriage (RM) cases. The study further investigated the potential use of these nanoparticles as a complementary treatment alongside antibiotics to overcome bacterial resistance.

Materials and Methods: ZnONPs were synthesized by mixing the *J. regia* bark extract with a zinc precursor solution, where a color change from brown to light yellow indicated nanoparticle formation. UV-Visible spectrophotometry confirmed the synthesis with an absorption peak at 192 nm. Functional groups responsible for the reduction and stabilization were identified by Fourier Transform Infrared Spectroscopy (FTIR), showing the presence of carboxylic and polyphenolic compounds. X-ray Diffraction (XRD) analysis revealed the crystalline nature of the nanoparticles with an average size of 13.8 nm. Scanning Electron Microscopy (SEM) showed elongated aggregated nanoparticles with one end wider than the other. X-Ray Fluorescence (XRF) analysis revealed that the zinc content in the ZnONPs reached 16.72% compared to 0.51% in the raw bark extract. Antibacterial activity was tested against bacterial isolates from RM cases, with inhibition zones measured at concentrations of 25, 50, and 100 mg/mL, and the minimum inhibitory concentration (MIC) determined.

Results: The biosynthesized ZnONPs showed strong antibacterial activity against the tested pathogens. The highest inhibition zones were recorded at all tested concentrations, with the MIC determined at 25 mg/mL. The antibacterial efficiency of ZnONPs was significantly enhanced by the phytochemicals in the *J. regia* bark extract, providing a potential alternative or complementary agent to conventional antibiotics against drug-resistant bacteria.

Conclusion: The study demonstrates that *J. regia* bark extract can be successfully used for the green synthesis of ZnONPs with potent antibacterial properties. These nanoparticles show promising potential as alternative or supplementary agents in the treatment of infections caused by multidrug-resistant bacteria, particularly in recurrent miscarriage cases. Further studies are recommended to explore their synergistic effects with antibiotics and their safety profile in biological systems.

Keyword: Zinc oxide nanoparticles (ZnONPs), *Juglans regia*, green synthesis, antibacterial activity, recurrent miscarriage (RM), multidrug-resistant bacteria, FTIR, XRD, SEM, XRF

1. INTRODUCTION:

Juglans regia commonly known as the English walnut, is a significant deciduous tree belonging to the Juglandaceae family. It is primarily recognized for its edible nuts and high-quality timber, making it one of the most economically important nut trees globally [1]. *J. regia*, commonly known as the walnut tree, exhibits significant antimicrobial properties that can inhibit the growth of various microorganisms, potentially preventing infections[2]. Research indicates that various parts of plants, including leaves, bark, and nuts, contain compounds with significant antimicrobial properties. These compounds can

effectively target a wide range of pathogens, including antibiotic-resistant strains [3]. Also for green synthesis of nanoparticles environmentally friendly methods for producing materials, often using biological organisms or natural processes. Some sources are used in the manufacture of nutrients for living organisms, including zinc [4]. In the context of using plant parts, various components can be utilized for synthesizing nanoparticles, pharmaceuticals, or other compounds [5]. Nanoparticles engineered from various materials such as metalloids, metallic oxides, non-metals, and carbon nanomaterials, have emerged as versatile agents in combating plant diseases. These nanoparticles generally range in size from 1 to 100 nm and exhibit unique properties that enhance their effectiveness in medicinal applications [6]. ZnONPs are garnering significant attention in the field of nanomedicine, particularly for their potential as next-generation nano antibiotics to combat multi-drug resistant pathogens. Their unique physicochemical properties, such as morphology, particle size, crystallinity, and porosity, contribute to their effectiveness against a broad spectrum of microorganisms [7]. The *J. regia* for leaves, bark, and nuts that contain bioactive compounds with these antimicrobial properties that can inhibit the growth or destroy various microorganisms responsible for infections [2 and 8].

The most common organism isolated was *E. coli*, *Klebsiella spp.* and *Enterobacter spp.* From recurrent miscarriage. Which is characterized by the consecutive loss of two or more pregnancies before reaching viability. Various factors may contribute to recurrent miscarriage by including advanced maternal age, lifestyle choices, genetic predispositions, both hereditary and acquired thrombophilia, and infections. Metabolic, endocrine, and anatomical factors such as uterine malformations have also been implicated as potential causes of RM. [9]. The role of ZnONPs in combating bacterial infections has garnered significant attention in recent years, particularly due to their potential as micro biostatic agents. These highlighting their ability to inhibit bacterial growth and to prevent the emergence of antimicrobial resistance AMR. Antimicrobial properties are influenced by a variety of factors, including particle size, and shape, concentration, more stability, time of exposure, pH, and surface properties [10]

2. MATERIALS AND METHODS:

i . Plant Collection and Identification:

In August and September 2024, the bark of *Juglans regia* (walnut) was collected from a specific location in Northern Iraq. This collection was part of a study aimed at exploring the properties of the bark., The plant specimen was identified in Plant Herbarium / Biology Department / College of Science / University of Babylon. The process of collecting, drying, and grinding bark into a fine powder (figure 1) is essential for preserving its beneficial properties and preparing it for various applications.



Figure(1): *J. regia* bark collection(a) and grinder(b)

ii. Preparing of Aqueous Bark Extract of *J. regia*:

The extraction process of *J. regia* bark was involved in creating an aqueous extract with 5% (w/v), by adding 5g of *J. regia* bark powder to 100 mL of high purity and sterility water, heating at 60 °C for 15-20 minutes, filtering it with What man filter paper No.1, and then storing it at 4 °C for future use [11].The storage not prolong for one day to maintain the texture of plant extract as possible .

iii. Synthesis of ZnONPs from *J.regia* bark extract:

Add 25 mL of bark extract dropwise to 100ml of $\text{ZnSO}_4 \cdot 7\text{H}_2\text{O}$ (0.1 M), after an 5 hour reaction period, a colour change occurred, indicating a chemical transformation. A blurry substance appeared, suggesting the formation of precipitates or complexes. The process described involves the synthesis and characterization of ZnONPs. Primary centrifugation at 6000 rpm for 15 minutes separates the precipitate removed, the filtrate was incubated for 24 hours, then drops of NaOH (1M) were added to the filtrate to adjust the pH to 11. It was noted that the colour of the solution changed to light yellow. Then, the centrifugation process was carried out at 6000 rpm for 15 minutes three times, and each time the precipitate was washed with distilled water. Then, the precipitate was collected and dried in the dark at laboratory temperature which represented the ZnONPs [12]. The dried precipitate is then analysed using several techniques to assess its properties. UV-Visible Spectrum, FTIR (Fourier Transform Infrared), XRD (X-Ray Diffractometer), *Field Emission Scanning Electron Microscope*

(FESEM) and X-ray fluorescence (XRF) . These techniques are important to determine the ZnONPs as in many research papers [13and 4]. The ZnONPs sample was compared with the *J.regia* bark extract sample alone within all experimental measurements for comparison.

iv. Bacterial samples collection and antibacterial susceptibility :

Isolated bacteria (*E. Coli*, *Klebseilla spp* and *Enterobacter spp.*) were obtained from women with recurrent miscarriage (cervical swab) from Babylon Teaching Hospital for Women and Children in Babylon. Using blood agar , MacConkey and chromogenic agar for isolation these bacteria (figure 2 a, b, c and d). The process of antibiotic susceptibility testing using the Kirby-Bauer method on Mueller Hinton Agar is a standard microbiological technique. This method assesses the effectiveness of various antibiotics against specific bacterial isolates were examined for antibiotic susceptibility. the samples were cultured on Mueller Hinton Agar . The plates were incubated at 37 °C for 24 hours. according to Clinical & Laboratory Standards Institute (14 and15) disk diffusion assay, with commonly used antibiotics in the hospital: Ciprofloxacin(5 µg) , Amikacin(30 µg) , Aztreonam (30 µg) , Ciprofloxacin (5 µg) , Levofloxacin(5 µg) , Nalidixic acid(30 µg), Nitrofurantion (300 µg) , Cefotaxime (30 µg)and Cefazidime (30µg) .[16].

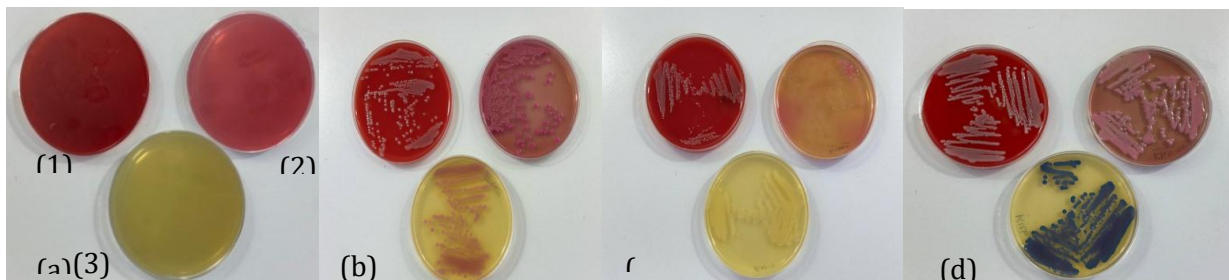


Figure (2): Bacterial isolation Using blood agar(1) , MacConkey(2) and chromogenic agar(3) for isolation of bacteria (a) control,(b) *E.coli*, (c) *Enterobacter sp.* and(d) *Klebsiella sp.*

v. Antimicrobial tests for nanoparticles:

The ZnONPs manufactured by the green synthesis method were tested against *E.coli*, *Klebseilla spp* and *Enterobacter spp.* These were done in addition to the agar diffusion method, Mueller- Hinton agar was used to evaluate the microbial susceptibility of ZnONPs. Mueller-Hinton agar was prepared according to the manufacturer's directions and poured into Petri dishes to reach a mean thickness of approximately 1.0 cm, autoclaved for 15 min at 121 C°, and then allowed to solidify. The overnight turbidity of *E.coli*, *Klebseilla spp* and *Enterobacter spp.* using the standard McFarland technique. A cotton swab was soaked in each microbial growth under investigation, wiped on the surface of Mueller-Hinton agar, The holes were then filled with 100 µl of ZnONPs prepared at six concentrations (3.12, 6.25, 12.5, 25, 50, and 100 mg/ml). All dishes were incubated for a 24 h, at a temperature of 37 C°, and the zones of inhibition were determined in(mm) for each sample to find which materials had the best antimicrobial activity [17] (figure 3) .

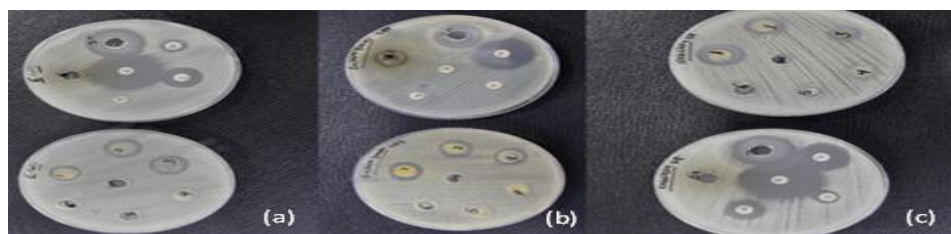


Figure (3): :Antimicrobial tests for nanoparticles and antibiotic IMP(10 µg),AMK(30 µg),CTX(30 µg),CFM(5 µg) (a) *E.coli*, (b) *Enterobacter sp.* and(c) *Klebsiella sp.*

vi. Minimum Inhibitory concentration (MIC):

The determination of MIC values is a critical aspect of microbiological research and clinical practice show in (figure 4), providing essential information on the efficacy of antimicrobial substances like *J. regia* bark extract and ZnONPs. This knowledge aids in optimizing treatment strategies and combating antimicrobial resistance effectively. In the context of this study, both the *J. regia bark* extract and the green synthesized ZnONPs evidenced antibacterial activity against *E. coli*, *KlebseiA spp.* and *Enterobacter spp.* isolates. MIC values were determined by testing range of concentration 25 mg/ml of the ZnONPs [18].

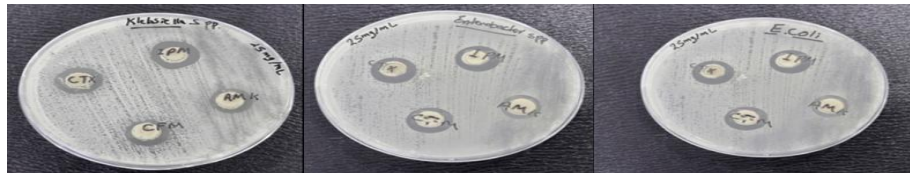


Figure (3): :Antimicrobial tests for nanoparticles and antibiotic IMP(10 µg),AMK(30 µg),CTX(30 µg),CFM(5 µg) (a) *E.coli*, (b) *Enterobacter sp.* and (c) *Klebsiella sp.*

vii. Statistical analysis

One-way ANOVA test was used to evaluate the inhibition zones of bacteria isolated from women with recurrent miscarriage at the significance level of 0.05 by the least significant difference (L. S. D.) via IBM SPSS v.24 software.

Ethical certification

The present study followed the principles of the Declaration of Helsinki. Before sample collection, verbal and written consent was obtained from the patients. A local ethics commission reviewed and approved the study protocol, consent form, and subject information on June 11, 2024, under project number M240601.

3. RESULTS

i. Colour changes:

The observed colour change from brown to yellow as shown in figure 5 a & b, accompanied by the formation of brown precipitation shortly after mixing $\text{ZnSO}_4 \cdot 7\text{H}_2\text{O}$ (0.1 M) with *J. regia* bark extract (5%), is indicative of the rapid synthesis of ZnONPs through a biological process. The change in colour is the initial stage of nanoparticle formation, which can occur within a 5-6 hr., the time of colour change differ depending on plant species for ZnONPs formation [19and 20].

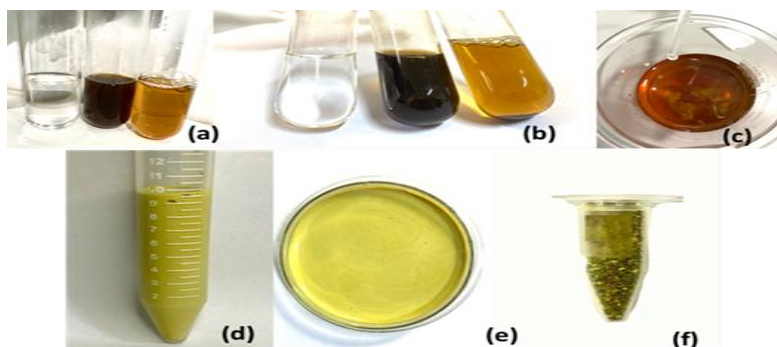


Figure (5): Synthesis of the ZnONPs from *J.regia* bark extract. Color change comparing between the mixture of *J. regia* bark extract addition NaOH (a ,b, and c).synthesis of ZnONPs (d,e&f).

ii. UV-visible Spectrum Analysis:

The optical properties of the synthesized ZnO nanoparticles (ZnONPs) were characterized using UV-visible spectrophotometry, within the wavelength range of 200–1200 nm, as shown in Figure 6. The UV-Vis spectrum of the synthesized ZnONPs (Figure 6) exhibited the highest absorption at 192 nm, while the *Juglans regia* bark extract showed a peak absorption at 220 nm. This shift in the absorption peak suggests that the ZnONPs are more stable in solution compared to the nanoparticles. Furthermore, the higher absorption intensity of the ZnONPs indicates better solubility and dispersion of the nanoparticles in the solution. The broad absorption bands observed in the UV-Vis spectrum of the *J. regia* bark extract point to a heterogeneous distribution in terms of particle size and shape. This contrasts with the relatively more uniform absorption profile of the ZnONPs, suggesting a more consistent nanoparticle structure.

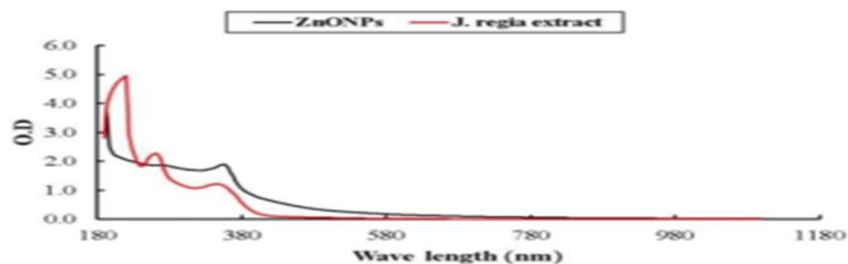


Figure (6): Absorption spectrum of synthesized ZnONPs by *Juglans regia* bark extract

iii. Fourier Transform Infrared (FTIR):

The FTIR spectra of *J. regia* bark extract and the synthesized ZnO nanoparticles (ZnONPs) are depicted in Figures 7(a ,b), respectively. The FTIR analysis of the ZnONPs, synthesized using bioactive compounds from the plant extract, revealed several significant absorption peaks between 4000 cm^{-1} and 400 cm^{-1} . These peaks indicate the presence of functional groups involved in the reduction and stabilization of ZnONPs. The specific absorption peaks observed in the FTIR spectrum of the ZnONPs include: 3435.71 cm^{-1} : Corresponding to the stretching vibrations of the O–H group, likely from phenolic compounds in the extract. 2067.09 cm^{-1} : Assigned to C–H stretching vibrations, suggesting the presence of aliphatic hydrocarbons or alkane structures in the extract. 1636.16 cm^{-1} : Associated with C=C stretching or N–H bending, indicating aromatic compounds or amino acids. 1310.44 cm^{-1} : Linked to C–C stretching in the aromatic ring. 1180.32 cm^{-1} , 1142.02 cm^{-1} , 1076.02 cm^{-1} : Corresponding to C–N stretching, suggesting nitrogen-containing compounds, such as amines. 995.60 cm^{-1} and 678.88 cm^{-1} : Associated with C–N stretching vibrations from amines. The comparison of the FTIR spectra of *J. regia* extract and ZnONPs indicates the involvement of the extract's bioactive compounds in the synthesis and stabilization of the nanoparticles. Additionally, two new peaks, 1096.19 cm^{-1} and 1015.99 cm^{-1} , appeared in the ZnONPs spectrum after purification, which can be attributed to C–O stretching vibrations.

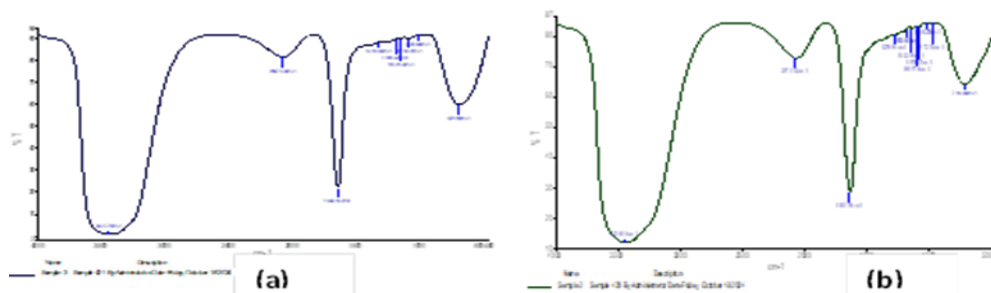


Figure 7: FTIR spectrum of biosynthesized (a) *J.regia* bark extract (b) ZnO NPs and

iv. X-ray Diffraction (XRD) Analysis:

The crystalline structure of the synthesized ZnO nanoparticles (ZnONPs) was analyzed using X-ray diffraction (XRD). As shown in Figure 8(a), the XRD pattern of the *Juglans regia* bark extract did not display any distinct diffraction peaks, indicating the absence of crystalline structures and suggesting that the material is in the initial stages of nanoparticle formation. The calculated average particle size from the extract was approximately 30.1 nm. In contrast, the XRD pattern of the synthesized ZnONPs, depicted in Figure 8(b), exhibited several sharp and narrow diffraction peaks at 31.5°, 35°, 37°, 47°, 57°, 63°, and 69° (2θ). The presence of these well-defined peaks confirms the formation of highly crystalline ZnO nanoparticles with a hexagonal wurtzite structure, characteristic of pure metallic ZnO nanoparticles. The average crystallite size of the ZnONPs was calculated using the Debye-Scherrer equation: $D = k\lambda / (\beta \cos \theta)$ Where: D = crystallite size , k = Scherrer's constant (0.9–1.0 for spherical particles) λ = X-ray wavelength , β = full width at half maximum (FWHM) of the diffraction peak, θ = diffraction angle Based on the most intense diffraction peak, the average crystallite size of the ZnONPs was determined to be 13.8 nm.

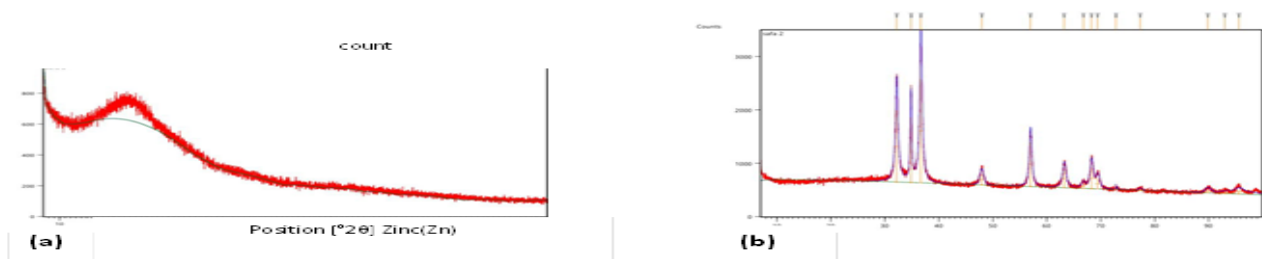


Figure 8 : X-ray diffraction (XRD) results for (a) *J.regia* bark extract and (b) ZnONPs

v. Scanning Electron Microscope (SEM) Analysis:

The surface morphology, particle size, and shape of the synthesized ZnO nanoparticles (ZnONPs) were examined using Scanning Electron Microscopy (SEM), providing detailed high-resolution images of the nanoparticles. As shown in Figure 9(a), the SEM image of *Juglans regia* bark extract revealed aggregated particles with an average diameter of 47.5 nm. These particles predominantly exhibited a spherical shape. In contrast, the SEM image of the synthesized ZnONPs Figure 9(b) showed that the nanoparticles were primarily present as elongated aggregated particles, characterized by one end being wider than the other. The average particle diameter of the ZnONPs was calculated to be 43.5 nm. The distinct change in particle morphology after synthesis is a notable observation.

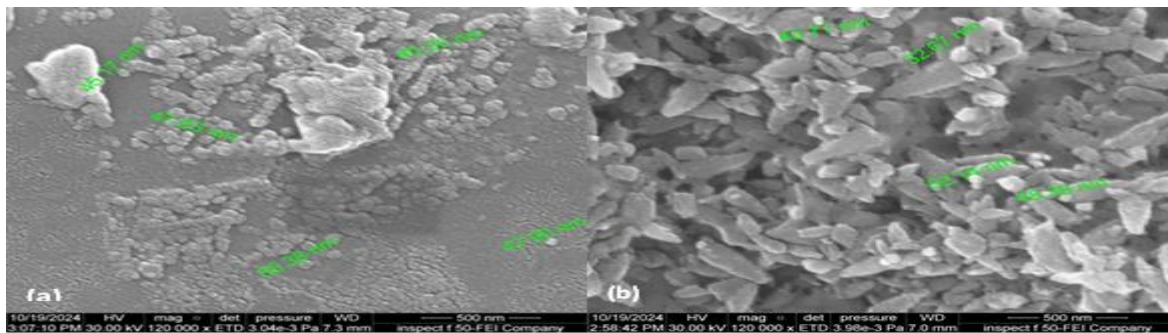


Figure9(a) : FESM of (a) *J.regia* bark extract and (b)ZnONPs

vi. X-ray fluorescence (XRF):

The analysis results using X-ray fluorescence (XRF) revealed the presence of the metallic elements in *Juglans regia* and zinc oxide nanoparticles (ZnONPs). As shown in Tables 7(a) and 7(b), it was confirmed that the percentage of most metals decreased when moving from the active extract to the different view, with the exception of zinc, which decreased significantly from 0.51% in the extract to 16.72% in the different view.

Table 1 : Chemical Analysis For *J.regia* bark extract (a) & ZnONPs (b)

<i>J.regia</i> bark extract(a)		ZnONPs (b)	
Element	Content	Element	Content
MgO(%)	0.44	MgO(%)	0.57
Al ₂ O ₃ (%)	30.88	Al ₂ O ₃ (%)	0.72
SiO ₂ (%)	1.41	SiO ₂ (%)	0.61
P(%)	0.22	P(%)	0.01
K(%)	1.32	K(%)	0.37
Ca(%)	0.78	Ca(%)	0.05
Fe(%)	0.01	Fe(%)	0.05
Ni(%)	0.02	Ni(%)	0.20
Zn(%)	0.51	Zn(%)	16.72
S(%)	0.12		

vii. Antimicrobial Activity and Inhibition Zone:

The antimicrobial activity of *Juglans regia* bark extract, zinc sulfate solution, and biosynthesized ZnO nanoparticles (ZnONPs) was evaluated against three bacterial isolates: *Klebsiella sp.*, *Escherichia coli*, and *Enterobacter sp.*, using the well diffusion method. The results are presented in Table 2. The *J. regia* bark extract (5%) exhibited a significant inhibitory

effect on the growth of all three tested bacterial species. ZnONPs showed concentration-dependent antibacterial activity. Higher concentrations (25–100 mg/ml) of ZnONPs demonstrated significant inhibition zones against all bacterial isolates compared to the control and lower concentrations (3.12–12.5 mg/ml). The statistical analysis confirmed that 25 mg/ml was the minimum concentration that produced the highest significant inhibition across the three bacterial species. Comparison with antibiotics revealed that *Enterobacter* spp. showed resistance to Imipenem (IPM), whereas *Klebsiella* sp. and *E. coli* were sensitive to IPM (10 µg). Additionally, the zinc sulfate solution alone produced a high and significant inhibition zone, comparable to the effect of IPM on *Klebsiella* spp. and *E. coli*.

vii. Minimum Inhibitory Concentration (MIC) Analysis:

Minimum inhibitory concentrations (MICs) refer to the lowest effective doses of antimicrobial substances that prevent the visible growth of microorganisms after an overnight incubation period. Alexander Fleming pioneered the concept of MIC by using broth turbidity to quantify the antibacterial activity of drugs. In the late 1980s, the Clinical and Laboratory Standards Association established standardized methods and criteria for determining MICs in clinical settings to evaluate the bacteriostatic effects of antibiotics. In the context of this study, both the *J. regia* bark extract and the green synthesized ZnONPs demonstrated antibacterial activity against *Klebsiella* spp., *E.coli* and *Enterobacter* spp. isolates. MIC values were determined by testing a range of concentrations of the ZnONPs in nutrient broth culture media are displayed in table 3. ZnONPs was selected at a concentration of 25 mg/ml after it caused the highest inhibition for each of the three bacterial species. This concentration was tested with antibiotics. It is noted that both combinations of 25 mg/ml of ZnONPs with the antibiotics CFM (30 µg) and CTX(30 µg) caused significant inhibition compared to CFM (5µg) and CTX(30µg) before adding ZnONPs for all bacterial species under study. *Enterobacter* sp. were resistant to the antibiotic IPM(10 µg), but after being treated with the combination of IPM (10µg) + ZnONPs (25 mg/ml), the inhibition zone enhanced (17.7 mm) comparing with the antibiotic AMK (30µg) alone. Table 3 data showed the combination between ZnONPs in concentration 25mg/ml lead to the three types of bacteria became susceptibility to CFM (5µg) and CTX (30µg) antibiotics. The formed ZnONPs and the ZnONPs (25 mg/ml) incorporated IPM (10µg), AMK(30µg), CFM(5µg) and CTX(30µg) displayed significant antibacterial activity against *Klebsiella* spp., *E.coli* and *Enterobacter* spp. (Figure 5).

Table (3) :Inhibition zone (mm) for isolated bacteria from recurrent miscarriage that are affected by combination of ZnONPs with antibiotic :

Treatments \ Bacteria	<i>E.coli</i>	<i>Klebsiella</i> <i>spp.</i>	<i>Enterobact</i> <i>er spp.</i>
Control	0	0	0
ZnONPs 25 mg/ml	17.7	18	16
IPM(10 µg)	25	28	0
AMK(30 µg)	11.3	15.7	22.7
CFM(5µg)	0	0	0
CTX(30 µg)	0	0	0
IPM (10µg)) +ZnONPs(25mg/ml)	17.7	19.3	17.7
AMK(30µg)+ZnoNPs(25mg/ml)	16.7	17.3	16.3
CFM(5µg)+ZnoNPs(25mg/ml)	17.7	17.3	18.3
CTX (30 µg) +ZnoNPs(25mg/ml)	17.7	18	18
LSD(0.05)	1.43	1.29	1.53

4. DISCUSSION

i. UV-visible Spectrum Analysis

The observed absorption peak of ZnONPs at 192 nm is indicative of the successful synthesis of nanoparticles, with enhanced stability and solubility in solution compared to the *J. regia* bark extract, which absorbed most strongly at 220 nm. The difference in absorption peaks suggests that the phytochemicals in the bark extract are involved in the reduction and stabilization of the ZnO nanoparticles, likely contributing to their distinct optical properties.[21] The broad absorption bands in the *J. regia* extract may reflect a wider distribution of sizes and shapes of the nanoparticles formed, which could influence their reactivity and interactions with bacterial cells. On the other hand, the narrower absorption band in the ZnONPs suggests that the synthesis process produced nanoparticles with more consistent characteristics, leading to enhanced dispersion and solubility. These findings underscore the utility of UV-visible spectrophotometry in characterizing the optical properties and stability of nanomaterials. The spectral differences also highlight the role of *J. regia* bark extract as both a reducing and

stabilizing agent during the green synthesis of ZnONPs.[22]

ii. Fourier Transform Infrared (FTIR) Spectral Analysis

The FTIR analysis revealed that several functional groups, such as hydroxyl groups (O–H), phenolic compounds, aliphatic hydrocarbons, and amines, were involved in the biosynthesis of ZnONPs.[23] The presence of these groups is crucial for the reduction of zinc ions and the stabilization of the nanoparticles. The peaks observed at 3435.71 cm^{-1} and 2067.09 cm^{-1} suggest that the bioactive compounds in *J. regia* bark extract, particularly phenolic compounds and aliphatic hydrocarbons, play a significant role in the reduction process, enabling the formation of stable ZnONPs. The 1636.16 cm^{-1} and 1310.44 cm^{-1} peaks further confirm the interaction between amino acids or aromatic compounds from the extract and the zinc ions. Moreover, the appearance of 1096.19 cm^{-1} and 1015.99 cm^{-1} peaks in the purified ZnONPs spectrum suggests that the interaction between the nanoparticles and oxygen-containing functional groups may contribute to their stabilization.[24] These findings emphasize the role of *J. regia* bark extract not only as a reducing agent but also as a stabilizing agent in the synthesis of ZnONPs. The FTIR spectra comparison indicates that the green synthesis method using plant extracts is effective in producing nanoparticles with distinct surface functionalization, contributing to the nanoparticles' enhanced stability and reactivity.[25].

iii. X-ray Diffraction (XRD) Analysis:

The absence of clear diffraction peaks in the *J. regia* bark extract confirms the non-crystalline, amorphous nature of the extract and supports its role as a reducing and stabilizing agent during nanoparticle formation. The sharp and intense peaks observed in the ZnONPs spectrum are indicative of the high purity and crystalline nature of the synthesized nanoparticles. [11]The calculated crystallite size of 13.8 nm falls within the nanoscale range, confirming successful synthesis of ZnONPs. The narrow peak widths further suggest the formation of uniform and well-crystallized nanoparticles. The XRD analysis not only confirms the purity and phase structure of the ZnONPs but also provides valuable information regarding particle size and crystallinity. These results highlight the effectiveness of *J. regia* bark extract in facilitating the biosynthesis of ZnONPs with desirable structural properties, making them suitable for potential biological and antimicrobial applications.[13].

iv. Scanning Electron Microscope (SEM) Analysis:

The SEM analysis confirmed the morphological transformation that occurs during the biosynthesis process. While the *J. regia* bark extract initially formed mostly spherical aggregates, the synthesized ZnONPs displayed a more elongated morphology with asymmetrical aggregation, suggesting that the reduction and stabilization process influenced the final nanoparticle shape. [26]The aggregation observed in both the extract and ZnONPs samples aligns with previous reports indicating the tendency of biologically synthesized nanoparticles to form clusters due to the presence of organic molecules acting as capping agents. Similar studies, such as those reported by [27] and [28], described spherical and aggregated nanoparticle structures when using *J. regia* bark extract. Additionally, the formation of larger aggregates alongside individual nanoparticles observed in the SEM images may be attributed to natural agglomeration during the drying or sample preparation process, which is commonly reported in green synthesis methods [29]. Overall, the SEM results highlight that the biosynthesis process not only reduces zinc ions but also impacts the morphological features of the resulting ZnONPs, producing nanoparticles with distinct elongated shapes potentially influencing their surface area and biological interactions.

v. X-ray fluorescence (XRF):

The highest percentage of zinc in the nano sample, which was the result of the successful technique followed by zinc oxide nanoparticles, reflecting the increased concentration and purity of zinc in the nano image.[31] Oxygen was also found associated with other elements, but in small proportions, indicating a significant interaction between the two elements during the chemical process. These results are compared with previous studies using XRF technology to accurately detect mineral elements in plant extracts and their proportions, which led to the production of the reliability of this technology in analytical studies on various plants[32].

vi. Antimicrobial Activity and Inhibition Zone:

The results clearly demonstrate the potent antibacterial activity of both *J. regia* bark extract and the biosynthesized ZnONPs. However, ZnONPs exhibited superior antibacterial efficacy, particularly at concentrations of 25 mg/ml and above, which is attributed to their nanoscale size and increased surface reactivity. These findings are consistent with previous studies [33], which highlighted the antibacterial and antioxidant properties of *J. regia* extract. Furthermore, the enhanced antibacterial effect of green-synthesized ZnONPs can be explained by their ability to interact more

effectively with bacterial cell membranes due to their small size, large surface area, and high reactivity. This interaction leads to membrane disruption, increased permeability, and ultimately, bacterial cell death. The observation that *Enterobacter sp.* was resistant to IPM but susceptible to ZnONPs suggests that green-synthesized ZnONPs could serve as a promising alternative or complementary agent to conventional antibiotics, especially in cases of antibiotic resistance. Moreover, the eco-friendly and cost-effective nature of the green synthesis approach adds value to the potential biomedical applications of

ZnONPs as effective antimicrobial agents against resistant bacterial strains.[34],

vii. Minimum Inhibitory Concentration (MIC) Analysis:

The MIC results highlight the potent antibacterial effect of biosynthesized ZnONPs, particularly at 25 mg/ml, against the studied multidrug-resistant bacterial isolates. The significant enhancement in inhibition zones upon combining ZnONPs with antibiotics supports the hypothesis that ZnONPs can act as effective antibiotic adjuvants. The ability of ZnONPs to restore the antibacterial activity of antibiotics like CFM and CTX, especially against resistant strains such as *Enterobacter sp.*, demonstrates their potential role in overcoming bacterial resistance mechanisms. The synergistic effect observed may be attributed to the nanoparticles' capacity to disrupt bacterial cell membranes, thereby increasing antibiotic penetration and efficacy. These findings align with previous studies, such as Madan [37], which reported similar synergistic interactions between green-synthesized ZnONPs and conventional antibiotics. This suggests that integrating ZnONPs with antibiotics could represent a promising strategy for enhancing antibacterial therapy against resistant pathogens.

5. CONCLUSIONS

1. The green synthesis of ZnONPs using *J. regia* bark is an eco-friendly and sustainable method that reduces the need for traditional chemical processes.
2. ZnONPs demonstrated effective antibacterial activity against *Klebsiella spp.*, *E. coli*, and *Enterobacter spp.* isolated from women with recurrent miscarriage.
3. A concentration of 25 mg/ml of ZnONPs, combined with antibiotics (CFM and CTX), successfully converted resistant bacteria to susceptible ones, including overcoming *Enterobacter sp.* resistance to IPM.

Recommendations:

1. Conduct further studies to understand the mechanism of action of ZnONPs in bacterial inhibition.
2. Assess the toxicity and safety of ZnONPs before clinical application.
3. Explore synergistic effects of ZnONPs with other antibiotics to enhance antibacterial activity.
4. Perform clinical trials to evaluate the efficacy of ZnONPs in treating bacterial infections

REFERENCES

- [1] .Shavvon, R. S., Qi, H. L., Mafakheri, M., Fan, P. Z., Wu, H. Y., Vahdati, F. B., Al-Shmgani, H. S., Wang, Y.-H., & Liu, J. Unravelling the genetic diversity and population structure of Persian Walnut in the Iranian Plateau, *BMC Plant Biology*, 2022 ,23, 201.
- [2] Elouafy, Y., El Yadini, A., Mortada, S., Hnini, M., Harhar, H., Khalid, A., Abdalla, A., Bouyahya, A., Goh, K. W., Ming, L. C., my el abbes, F., & Tabyaoui, M., Antioxidant, antimicrobial, and α -glucosidase inhibitory activities of saponin extracts from walnut (*Juglans regia* L.) leaves , *Asian Pacific Journal of Tropical Biomedicine*, 2032, 13(2), 60.
- [3] Mateş, L., Rusu, M. E., & Popa, D. S.). Phytochemicals and biological activities of walnut septum: A systematic review. *Antioxidants*, 2023; 12(3), 60.
- [4] Alrubaie, E. A.A. &Kadhim, R. E. Synthesis of ZnO nanoparticles from olive plant extract. *Plant Archives*, 2019;19(2): 339-344.
- [5] Rafique, M.; Tahir, R.; Gillani, S.S.A.; Tahir, M.B.; Shakil, M.; Iqbal, T.; Abdellahi, M.O. Plant-mediated green synthesis of zinc oxide nanoparticles from *Syzygium cumini* for seed germination and wastewater purification. *Int. J. Environ. Anal. Chem.* 2022, 102, 23–38.
- [6] Khan, I.; Saeed, K.; Khan, I. Nanoparticles: Properties, applications and toxicities. *Arab. J. Chem.* 2019, 12, 908–931.
- [7] Silva B.L., Abuçafy M.P., Berbel Manaia E., Oshiro Junior J.A., Chiari-Andréo B.G., Pietro R.C.R., Chiavacci L.A. Relationship Between Structure And Antimicrobial Activity Of Zinc Oxide Nanoparticles: An Overview. *Int. J. Nanomed.* 2019;14:9395–9410.
- [8] Żurek, N., Pawłowska, A., Pycia, K., Grabek-Lejko, D., & Kapusta, I. T. Phenolic profile and antioxidant, antibacterial, and antiproliferative activity of *Juglans regia* L. male flowers. *Molecules*, 2022; 27(9), 2762.
- [9] Tsonis, O.; Balogun, S.; Adjei, J.O.; Moge kwu, O. and Iliodromiti, S. Management of recurrent miscarriages: an overview of current evidence. *Curr Opin Obstet Gynecol.* 2021;Oct 1;33(5):370-377.
- [10] .Abdelghafar, N Yousef, M Askoura - *BMC microbiology*, - Springer. Zinc oxide nanoparticles reduce biofilm

formation, synergize antibiotics action and attenuate *Staphylococcus aureus* virulence in host; an important message ,2022.

- [11] Vaishnava, J.; Subhaa, V.; Kirubanandana, S.; Arulmozhib,M. and Renganathana, S. Green synthesis of zinc oxide nanoparticles by celosia Argentea and its characterization. *Journal of Optoelectronics and Biomedical Materials.*, 2017; 9(1): 59 – 71.
- [12] Hoseyni, S. J.; Manoochehri, M. & Asli, M. D. Synthesis of cobalt nanoparticles by complex demolition method using the reaction between organic ligand Schiff base and cobalt chloride by ultra-sonication. *Bulletin de la Société Royale des Sciences de Liège*, 2017;86: 325-331.
- [13] Kadhim, R. E. & Abd, S. Y. Synthesis of copper nanoparticles biologically by *Conocarpus erectus* L. aqueous leaves extract. *Journal of University of Babylon*, 2018;26(5): 95-102.
- [14] Gaur, P., Hada, V., Rath, R. S., Mohanty, A., Singh, P., & Rukadikar, A. Interpretation of antimicrobial susceptibility testing using European Committee on Antimicrobial Susceptibility Testing (EUCAST) and Clinical and Laboratory Standards Institute (CLSI) breakpoints: analysis of agreement. *Cureus*, (2023). 15(3).
- [15] Giske, C. G., Turnidge, J., Cantón, R., & Kahlmeter, G. Update from the European committee on antimicrobial susceptibility testing (EUCAST). *Journal of clinical microbiology*, (2022). 60(3), e00276-21.
- [16] Vasconcelos, A. C. F. D., Stedefeldt, E., & Frutuoso, M. F. P. Uma experiência de integração ensino-serviço e a mudança de práticas profissionais: com a palavra, os profissionais de saúde. *Interface-Comunicação, Saúde, Educação*, (2016). 20, 147-158.
- [17] M.J. Tuama, M.F.A. Alias, Synthesis and characterization of zirconium oxide nanoparticles using *Z. officinale* and *S. aromaticum* plant extracts for antibacterial application, *Karbala Int J Modern Sci* 2023;9 698e711
- [18] Taraneh Movahhed, Maryam Mehrabkhani, Mohsen Arefnezhad, Shokouh Sadat Hamed, Reza Zare Mahmoudabadi, Fariba Ghanbari, Mahjubeh Rostami, Antibacterial Efficacy of Walnut Green Husk (WGH) Extract with Zinc Oxide Nanoparticles on *Streptococcus Mutans*, *Reports of Biochemistry & Molecular Biology*, 2022, Oct ,11, 3.
- [19] Jayandran, M., Haneefa, M. M., & Balasubramanian, V. Green synthesis and characterization of Manganese nanoparticles using natural plant extracts and its evaluation of antimicrobial activity. *Journal of Applied Pharmaceutical Science*, 2015;5(12), 105-110.
- [20] Alaa Imad Khadhim and Rihab Edan Kadhim Synthesis of Cobalt Nanoparticles Biologically by *Conocarpus erectus* L. Aqueous Leaves Extract ,*Annals of R.S.C.B.*, 2021, 1583-6258, Vol. 25, Pages. 5361 – 5372.
- [21] Murali, M.; Kalegowda, N.; Gowtham, H. G.; Ansari, M. A.; Alomary, M. N.; Alghamdi, S.; Amruthesh, K. N. Plant-Mediated Zinc Oxide Nanoparticles: Advances in The New Millennium Towards Understanding Their Therapeutic Role in Biomedical Applications. *Pharmaceutics*. 2021;13(10): 1662.
- [22] Abirami, N.; Arulmozhi, R.; Siddharth, A. G. S. Plant Mediated Synthesis, Characterization of Zinc Oxide Nanoparticles using *Simarouba glauca* and its Antibacterial Activities. *Research Journal of Pharmacy and Technology*. 2020; 13(4): 1819-1824.
- [23] Devendran, G. and Balasubramanian, U. Qualitative phytochemical screening and GC-MS analysis of *Ocimum sanctum* L. leaves. *Asian Journal of Plant Science and Research.*, 2011; 1(4) : 44-48.
- [24] Awwad, A.M.; Albiss, B. and Ahmad, A.L. Green synthesis, characterization and optical properties of zinc oxide nanosheets using *Olea europaea* leaf extract. *Adv Mater Lett.*, 2014; 5 :520–524.
- [25] Liang, W.H. Green synthesis, characterization of zinc oxide nanoparticles and their photocatalytic activity. *Bachelor of Science a thesis of University Tunku Abdul Rahman* 2016.
- [26] Vidya, C.; Hiremath, S.; Chandraprabha, M.N.; Lourd Antonyraj, M.A.; Gopal, I.V.; Jain, A. and Bansala, K. Green synthesis of ZnO nanoparticles by *Calotropis Gigantea*. *Int. J. Curr.*, 2013; 1 : 118-120.
- [27] Helen, S.M. and Rani, M.H.E. Characterization and antimicrobial study of nickel nanoparticles synthesized from *dioscorea* (Elephant Yam) by green route. *International Journal of Science and Research.*, 2015; 4(11):216–219
- [28] Yovino, L., Kim, G., Ghorpade, R., Elsamra, R. M., & Vasu, S. Measurements of laminar burning speeds in ammonia and hydrogen-air mixtures for gas turbines. In *AIAA SCITECH 2023 Forum* (p. 1823).
- [29] Vidya, C., Hiremath, S., Chandraprabha, M. N., Antonyraj, M. L., Gopal, I. V., Jain, A., & Bansal, K. Green synthesis of ZnO nanoparticles by *Calotropis gigantea*. *Int J Curr Eng Technol*, (2013). 1(1), 118-120.
- [30] Ingerle, D., Pepponi, G., Meirer, F., Wobraschek, P., & Strel, C. (2016). JGIXA—A software package for the calculation and fitting of grazing incidence X-ray fluorescence and X-ray reflectivity data for the

characterization of nanometer-layers and ultra-shallow-implants. *Spectrochimica Acta Part B: Atomic Spectroscopy*, 118, 20-28.

- [31] Towett, E. K., Shepherd, K. D., Tondoh, J. E., Winowiecki, L. A., Lulseged, T., Nyambura, M., ... & Cadisch, G. (2015). Total elemental composition of soils in Sub-Saharan Africa and relationship with soil forming factors. *Geoderma Regional*, 5, 157-168.
- [32] Montanha, G. S., Rodrigues, E. S., Marques, J. P. R., de Almeida, E., Colzato, M., & Pereira de Carvalho, H. W. (2020). Zinc nanocoated seeds: an alternative to boost soybean seed germination and seedling development. *SN Applied Sciences*, 2(5), 857.
- [33] Barekat, S.; Nasirpour, A.; Keramat, J.; Dinari, M.; Meziame-Kaci, M.; Paris, C.; Desobry, S. Phytochemical composition, antimicrobial, anticancer properties, and antioxidant potential of green husk from several walnut varieties (*Juglans regia* L.). *Antioxidants* 2023, 12, 52.
- [34] Yaseen, S. M., Abid, H. A., Kadhim, A. A. , Aboglida, E. E. Antibacterial Activity of Palm Heart Extracts Collected from Iraqi Phoenix *Dactylifera* L. *Journal of Techniques*. 2019; 1: 52-59.
- [35] Ifeanyichukwu, U. L.; Fayemi, O. E.; and Ateba, C. N. Green synthesis of zinc oxide nanoparticles from pomegranate (*Punica granatum*) extracts and characterization of their antibacterial activity. *Molecules*. 2020; 25(19): 4521.
- [36] Doğan, S. Ş.; Kocabaş, A. Green synthesis of ZnO nanoparticles with *Veronica multifida* and their antibio film activity. *Human and Experimental Toxicology*. 2020; 39(3): 319-327.
- [37] ..Sayyar Z, Jafarizadeh-Malmiri H. Preparation of curcumin nanodispersions using subcritical water–Screening of different emulsifiers. *Chem Eng Technol*. 2020;43:263–72.

..
